

# Magnetic resonance imaging of the prostate: an overview for radiologists\*

*Ressonância magnética da próstata: uma visão geral para o radiologista*

Ronaldo Hueb Baroni<sup>1</sup>, Maria Ines Novis<sup>2</sup>, Ângela Hissae Motoyama Caiado<sup>3</sup>,  
Luciana Mendes de Oliveira Cerri<sup>1</sup>, Claudia da Costa Leite<sup>4</sup>, Giovanni Guido Cerri<sup>5</sup>

**Abstract** Prostate adenocarcinoma is the second tumor in incidence and mortality among malignant neoplasms in men. The differentiation between tumors confined to the organ and those with extraprostatic extension is critical for an appropriate therapeutic planning. Different studies have demonstrated that magnetic resonance imaging of the prostate with endorectal coil is useful in the local staging of these tumors. The present article presents information on the prostate gland anatomy, the tumor aspect at magnetic resonance imaging, specific signs of extracapsular extension and seminal vesicles invasion, protocol suggestions, general principles and relevance of proton spectroscopy, perfusion and diffusion imaging, role of magnetic resonance imaging in the postoperative and post-radiotherapy detection of local tumor recurrence, and also in the detection of lesions in patients with clinical/laboratory suspicion of prostate adenocarcinoma. Additionally, the present article describes differential diagnoses and limitations of the method.

**Keywords:** Prostate cancer; Adenocarcinoma; Magnetic resonance imaging; Cancer staging.

**Resumo** O adenocarcinoma prostático é o segundo tumor em incidência e mortalidade dentre as neoplasias malignas masculinas. Para adequada programação terapêutica é importante a distinção entre tumores confinados à próstata e aqueles com extensão extraprostática. Diferentes estudos têm demonstrado que a ressonância magnética da próstata com bobina endorretal auxilia no estadiamento local destes pacientes. Este artigo apresenta informações sobre a anatomia prostática, o aspecto tumoral à ressonância magnética, sinais de extensão tumoral extraprostática e invasão de vesículas seminais, sugestões de protocolo, princípios gerais e importância da espectroscopia de prótons, do estudo perfusional e da difusão, indicações da ressonância magnética na investigação de recidiva pós-operatória e pós-radioterapia, seu papel na detecção de lesões suspeitas em pacientes com suspeita clínico-laboratorial de adenocarcinoma prostático, além de apresentar os diagnósticos diferenciais e limitações do método.

**Unitermos:** Neoplasias da próstata; Adenocarcinoma; Imagem por ressonância magnética; Estadiamento de neoplasias.

Baroni RH, Novis MI, Caiado AHM, Cerri LMO, Leite CC, Cerri GG. Magnetic resonance imaging of the prostate: an overview for radiologists. *Radiol Bras.* 2009;42(3):185–192.

## INTRODUCTION

Prostate adenocarcinoma (PCa) is the second tumor in incidence and mortality among the malignant neoplasms in men,

surpassed only by non-melanoma skin cancer in incidence, and by lung cancer in number of deaths<sup>(1,2)</sup>.

The methods employed in the screening for PCa in the population are prostate-specific antigen (PSA) test and digital rectal examination. Transrectal ultrasonography-guided biopsy is the method of choice for histological diagnosis of the disease.

An accurate staging of the disease is of paramount importance for an appropriate therapeutic planning. The nomograms introduced by Partin combine clinical staging based on digital rectal examination,

PSA levels and the Gleason score determined by biopsy (the highest the Gleason score, the highest is the tumor aggressiveness), with a relatively high accuracy in local staging of PCa<sup>(3)</sup>.

Several studies have demonstrated that magnetic resonance imaging (MRI), with its high anatomical resolution, adds relevant information to the clinical nomograms in the local staging of PCa. Endorectal coil MRI presents an accuracy of 85% in the prediction of extracapsular extension and up to 97% for seminal vesicles invasion<sup>(4,5)</sup>.

New prospects include the 3 tesla MRI, that may be utilized with endorectal coil (possibly increasing even further the sensitivity and specificity in the local staging of PCa), or without the endorectal coil with

\* Study developed at Instituto de Radiologia do Hospital das Clínicas da Faculdade de Medicina da Universidade de São Paulo (InRad/HC-FMUSP), São Paulo, SP, Brazil.

1. PhDs, Physician Assistants at Instituto de Radiologia do Hospital das Clínicas da Faculdade de Medicina da Universidade de São Paulo (InRad/HC-FMUSP), São Paulo, SP, Brazil.

2. MD, Fellow PhD degree, Instituto de Radiologia do Hospital das Clínicas da Faculdade de Medicina da Universidade de São Paulo (InRad/HC-FMUSP), São Paulo, SP, Brazil.

3. Physician Assistant at Instituto de Radiologia do Hospital das Clínicas da Faculdade de Medicina da Universidade de São Paulo (InRad/HC-FMUSP), São Paulo, SP, Brazil.

4. Private Docent, Professor at Instituto de Radiologia do Hospital das Clínicas da Faculdade de Medicina da Universidade de São Paulo (InRad/HC-FMUSP), São Paulo, SP, Brazil.

5. Titular Professor, Division of Radiology, Chief of the Radiology Service at Instituto de Radiologia do Hospital das Clínicas da Faculdade de Medicina da Universidade de São Paulo (InRad/HC-FMUSP), São Paulo, SP, Brazil.

Mailing address: Dr. Ronaldo Hueb Baroni, Avenida Albert Einstein, 627/701, 4º andar, Bloco D, Morumbi. São Paulo, SP, Brazil, 05651-901. E-mail: rbaroni@gmail.com

Received May 7, 2008. Accepted after revision January 12, 2009.

consequential reduction in discomfort for the patient<sup>(6,7)</sup>.

The present study is aimed at presenting the most relevant aspects of the evaluation of the prostate by means of MRI, particularly those related to the detection and staging of PCa.

## ANATOMY

### Zonal anatomy of the prostate

The prostate is an inverted cone-shaped gland with the base adjacent to the vesical floor and the apex postero-inferior to the pubic symphysis. It is divided into four glandular zones: peripheral, transitional, central and periurethral<sup>(8)</sup>. The transitional, central and periurethral zones, hardly differentiated by imaging methods, are jointly denominated central gland. The limit between the peripheral zone and the central gland is called “surgical capsule”, and the

discontinuous fibromuscular layer covering the gland is the “prostatic capsule” (Figure 1). For a better localization of lesions and biopsy guidance, the prostate is conventionally divided into three regions by imaginary cross sectional lines (base, middle and apex), and in two sides by an imaginary longitudinal median line (left and right), thus configuring the prostatic sextants.

### Seminal vesicles

Normal seminal vesicles present a typical ductal pattern and hyperintense signal on MRI T2-weighted sequences.

## DESIGN AND OPTIMIZATION OF THE PROTOCOL

### General recommendations

A four-hour fasting and rectal preparation is recommended for greater comfort of the patient. Shortly before the examination

1 mL of N-butylscopolamine (20 mg/mL) shall be administered to reduce intestinal peristalsis.

### Study of the pelvis

The images shall be obtained from the aortic bifurcation to the lower limit of the pubic symphysis, utilizing the torso or pelvic phased-array coil.

**Suggested protocol** – Axial T2-weighted fast spin echo (FSE) with fat saturation, and axial T1-weighted gradient echo (GRE), 7 mm slice thickness, 1–2 mm interslice gap, 256 × 192 matrix, number of excitations (NEX) = 3 for T2-weighted sequences, NEX = 1 for T1-weighted sequences, field-of-view (FOV) of approximately 30 cm.

### Study of the prostate

Initially, the patients shall be given an explanation about the procedure. After that, a digital rectal examination is performed to evaluate the prostate size to guide an appropriate positioning of the coil. The coil (which is disposable) is covered by a condom and lubricated with local anesthetic gel (xylocaine). After the coil is in place, it is filled with 40 to 80 ml of air or perfluorocarbon, with the objective of keeping the coil in place and reducing sphincter contraction artifacts. Perfluorocarbon is preferred in examinations with spectroscopy, and its advantages will be further detailed.

The protocol for specific study of the prostate and seminal vesicles after endorectal coil insertion must comprise high-resolution FSE T2-weighted sequences in the axial, coronal and sagittal planes, from the bottom of the seminal vesicles to the prostate apex (Figure 2).

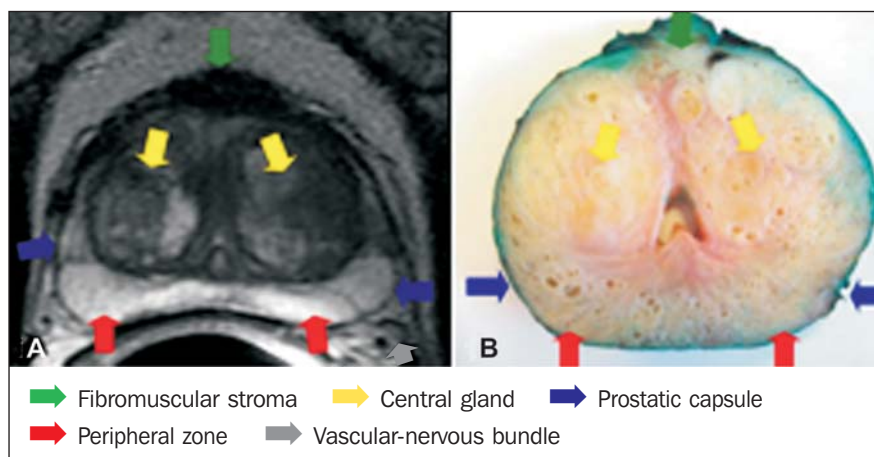


**Figure 1.** Correlation between MR T2-weighted image (A) and macroscopic aspect of a surgical specimen (B).

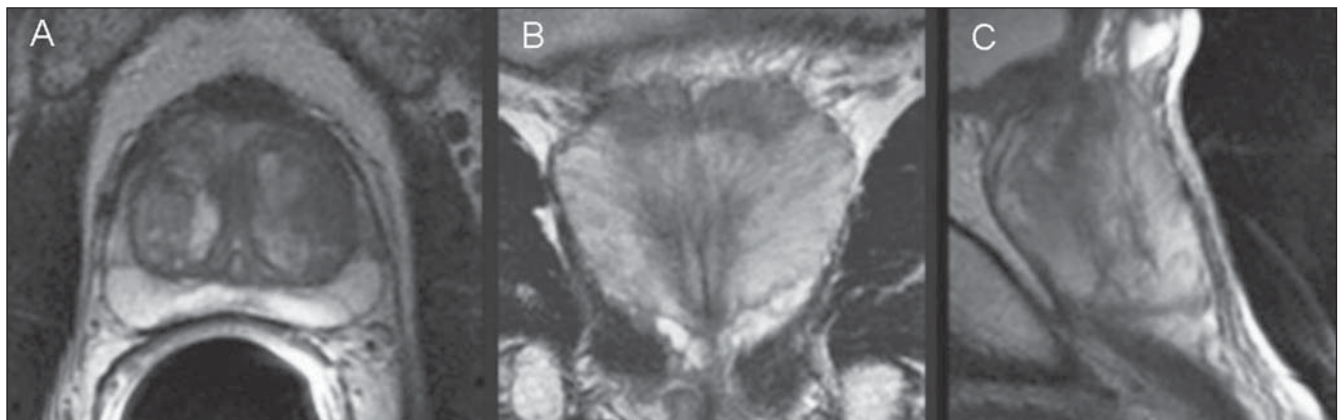


**Figure 2.** Endorectal coil MR, high-resolution T2-weighted images – axial (A), coronal (B), and sagittal (C) planes.

**Suggested protocol** – The sequences may be performed with 3–4 mm thick slices, 0–1 mm interslice gap, FOV from 12 to 16 cm, 256 × 256 matrix, NEX = 3 or 4 and TE = 120–160.

**TUMOR STAGING**

**Pathological staging**

The systems accepted for PCa staging are TNM and Jewett-Whitmore, TNM being the most widely utilized. The TNM classification describes the primary tumor extent (T), presence or absence of locoregional lymph node involvement (N) and presence or absence of metastases (M)<sup>(9)</sup>.

The appropriate preoperative PCa staging presents therapeutic and prognostic implications. Specifically, the detection of extracapsular extension and seminal vesicles invasion are of great importance, as they allow the differentiation between T2 and T3 stages<sup>(10)</sup>.

**Local staging – MRI**

**Tumor identification** – PCa is most frequently found in the peripheral zone (65%

to 74%). Usually the lesion presents like a poorly defined nodule with hypointense signal intensity on T2-weighted sequences, in contrast with signal hyperintensity in the normal peripheral zone (Figure 3).

**Detection of extracapsular extension**

– The detection of extracapsular extension can be inferred from both specific and non-specific signs at MRI<sup>(11)</sup>.

*Specific signs of extracapsular extension* (Figure 4): solid tissue in the periprostatic fat; irregular bulging of the prostatic capsule; obliteration of the rectoprostatic angle.

capsule; obliteration of the rectoprostatic angle.

*Non-specific signs of extracapsular extension:* regular capsular thickening; capsular discontinuity; regular bulging of the prostatic capsule.

**Invasion of seminal vesicles** – Invasion of seminal vesicles may occur by direct extension of the tumor localized in the base of the prostate gland, through the ejaculatory duct, or by hematogeneous spreading (Figure 5).

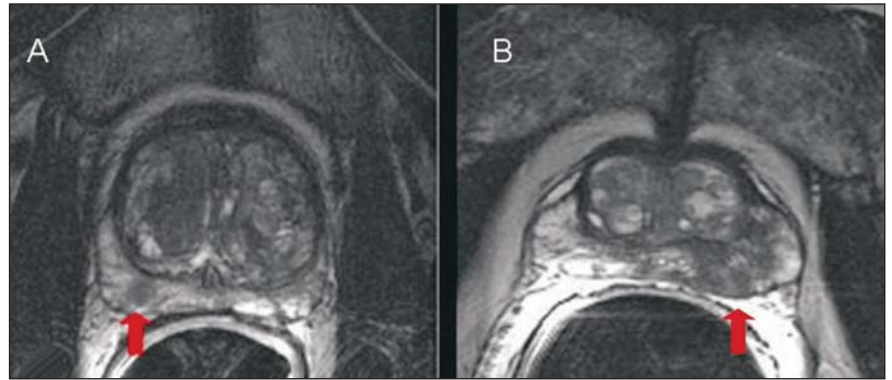


**Figure 3.** Endorectal coil MR – axial T2-weighted images depicting examples of nodular (A) and poorly defined (B) PCa.

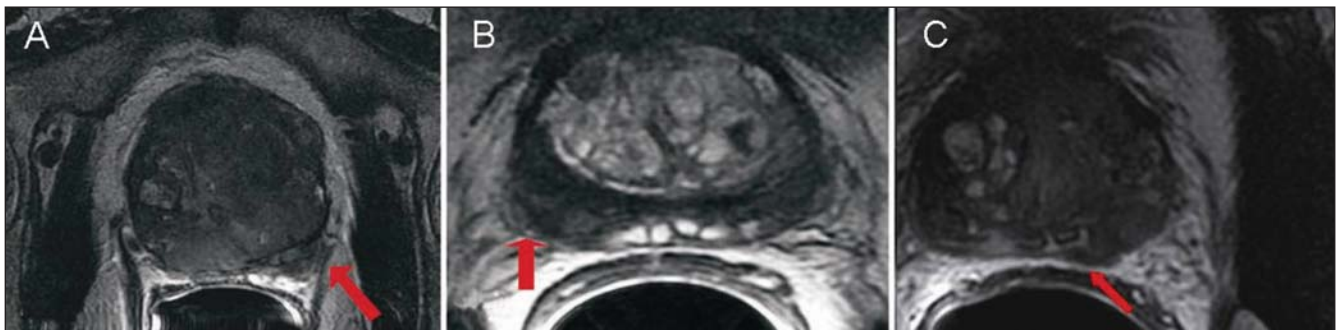


**Figure 4.** Endorectal coil MR – axial T2-weighted images demonstrating examples of PCa with extracapsular extension appearing as solid extraprostatic tissue (A), irregular capsular contour bulge (B) and rectoprostatic angle obliteration (C).

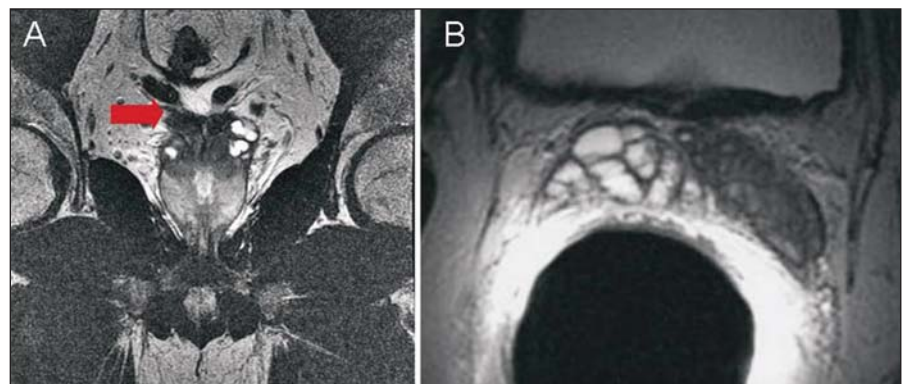


**Figure 5. A:** MR coronal T2-weighted image demonstrating PCA invading the seminal vesicles by contiguity. **B:** MR axial T2-weighted image demonstrating extensive tumor canalicular invasion of the left seminal vesicle through ejaculatory ducts.

Diagnostic findings of seminal vesicle invasion are: hypointense signal on T2-weighted sequences and loss of the typical ductal pattern<sup>(12)</sup>.

### Regional staging

It is also important to evaluate the sequences of the pelvis and of the prostate in the search for regional lymphadenopathies (> 1 cm in the smallest diameter), invasion of periprostatic structures and bone lesions (Figure 6).

## SPECTROSCOPY

### General principles

Proton spectroscopy allows a noninvasive evaluation of anatomic and biological characteristics of the tumor, emphasizing the detection, localization and staging of PCa. Spectroscopy utilizes a powerful magnetic field and radiofrequency waves to obtain metabolic data, based on the relative concentration of endogenous prostatic metabolites. It is always performed in association with endorectal coil MRI, increasing total examination time by 10 to 17 minutes.

Voxels of 0.3 cm<sup>3</sup> are programmed in the whole prostate extent, utilizing T2-weighted images as a reference, which allows the joint analysis of anatomical and metabolic alterations. The metabolites analyzed are: choline, creatine, citrate and, more recently, polyamine. The analysis is performed by means of amplitude  $\times$  frequency graphs, the frequencies being specific for each metabolite. The areas under the peaks correlate with the concentration of each metabolite in the prostatic tissue<sup>(13,14)</sup> (Figure 7).

**Citrate** – peak: 2.6 ppm. Metabolite synthesized by a healthy prostate, most remarkably in the peripheral zone. Hyperplastic nodules may present citrate levels as high as those observed in the peripheral zone. In the presence of cancer, citrate levels are reduced or undetectable.

**Choline** – peak: 3.22 ppm. Cell metabolism marker. Increased choline levels are observed in malignant tissues, because of high phospholipid metabolism of the cell membrane.

**Creatine** – peak: 3.03 ppm. Energy reserve with constant concentration. Because

of the proximity between creatine and choline peaks, they may be inseparable on the spectral line; therefore, the (choline + creatine)/citrate ratio is utilized in the spectral analysis. (Choline + creatine)/citrate ratios > 0.5 are suggestive of malignancy (the higher the ratio, the higher is the possibility of cancer).

**Polyamine** – peak: 3.1 ppm. This peak resolution is better observed when the endorectal coil is filled with perfluorocarbon. It is reduced in suspicious areas,

being identified as an acute decreasing curve between the choline and creatine peaks.

Perfluorocarbon, a fluorine and carbon compound without hydrogen atoms, can be utilized to inflate the endorectal coil, reducing the magnetic susceptibility difference between the air and the prostatic tissue. It improves the characterization of peaks of low spectral signals in the peripheral zone, as well as the peak resolution of each metabolite<sup>(15)</sup>.

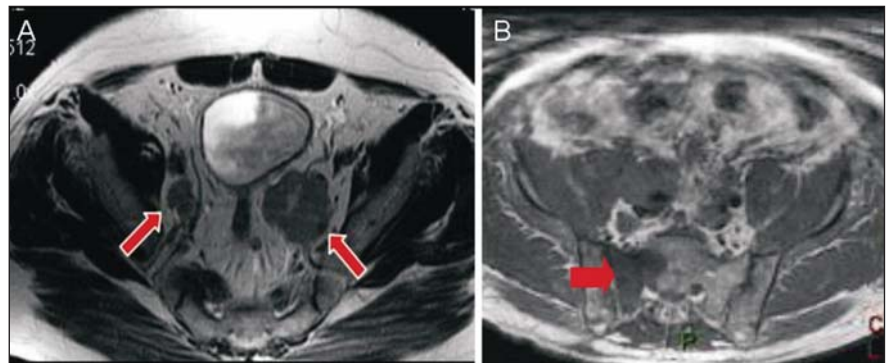


**Figure 6. A:** MR axial T2-weighted image demonstrating bilateral obturator lymphadenopathy. **B:** MR axial T2-weighted image demonstrating a metastatic bone lesion in the sacrum.

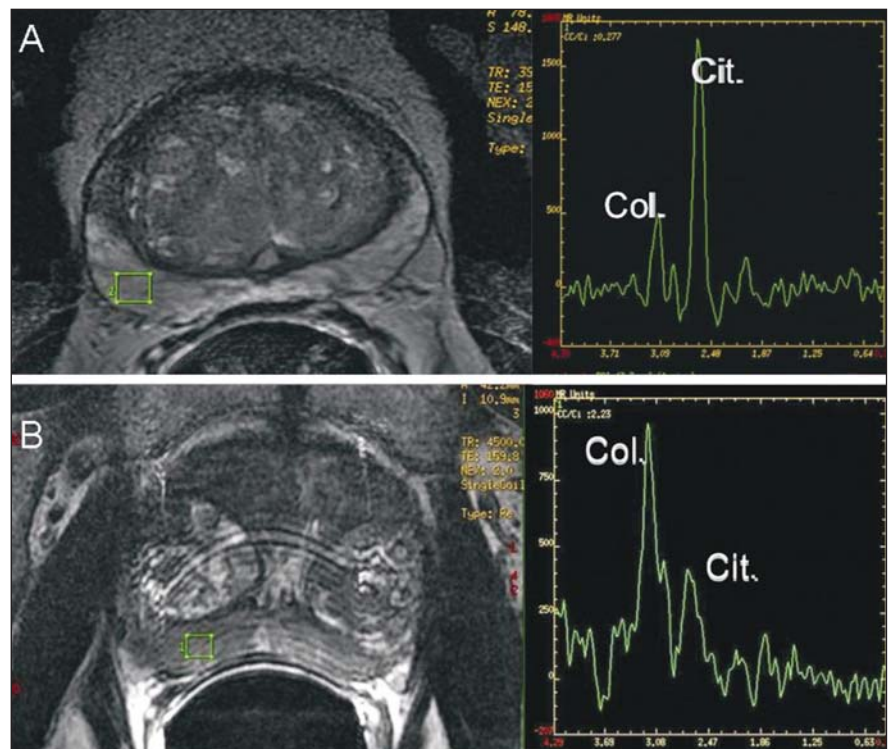


**Figure 7. A:** Normal peripheral zone, with high signal-intensity on MR axial T2-weighted image, and with a spectral graph demonstrating low choline and high citrate levels **B:** PCa in the peripheral region, with low signal-intensity on MR axial T2-weighted image, and spectral graph showing high choline and low citrate levels.

Jung et al.<sup>(16)</sup> described a score system in an attempt to standardize and systematize the prostatic metabolic evaluation. This five-score system utilizes progressively more suspicious spectral patterns, with good accuracy (74.2% to 85.0%) and excellent interobserver agreement, using a score  $\geq 4$  for tumor detection. Additional criteria, such as polyamine peak inversion, should be considered.

### Role of proton spectroscopy

**To increase the MRI specificity** – Lesions with hypointense signal on T2-weighted sequences may be observed in other non-tumor conditions such as hemorrhage and chronic prostatitis, among others. The addition of spectroscopy to endorectal coil MRI increases specificity and reduces interobserver variability<sup>(17)</sup>.

**To improve local staging (number of tumor voxels  $\times$  risk for extracapsular extension)** – Studies demonstrate that the higher the number of tumor voxels at spectroscopy, the higher is the risk for extracapsular extension. Patients with small tumors at MRI spectroscopy (0–1 tumor voxel/slice) presented a risk of 6% for extracapsular extension, while those with extensive tumors ( $> 4$  tumor voxels/slice) presented a risk of 80%<sup>(18)</sup> (Figure 8).

**To predict tumor aggressiveness** – MRI spectroscopy has the potential to noninvasively infer tumor aggressiveness. Tumor changes vary from a subtle increase in choline levels and moderate citrate levels in low grade tumors, to a sharp rise in choline levels and reduction/absence of citrate in high grade tumors<sup>(19)</sup>.

**To predict tumor volume** – Three-dimensional spectroscopy in combination with MRI increases global accuracy of tumor volume estimates. The prediction of tumor volume by MRI spectroscopy in lesions  $> 0.5 \text{ cm}^3$  obtained a significant correlation with histopathologic tumor volume<sup>(20)</sup>.

### PERFUSION STUDY (DYNAMIC CONTRAST-ENHANCED MRI)

Dynamic contrast-enhanced MRI is useful in the detection of areas under suspicion for neoplastic involvement. It is performed with 3D T1-weighted sequences, before

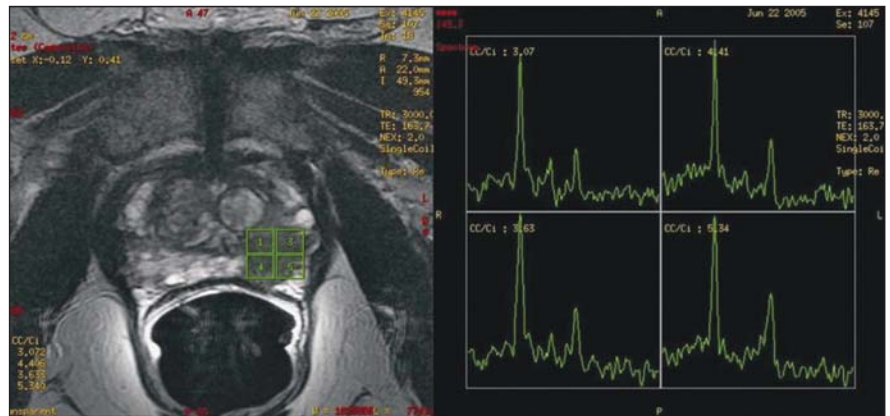


**Figure 8.** MR axial T2-weighted image demonstrating a lesion with low signal-intensity on the left apical peripheral zone, and four contiguous voxels with a neoplastic spectral pattern (increased choline and decreased citrate levels).

and after intravenous gadolinium injection (0.1 mmol of gadopentate dimeglumine/kg of weight), administered by injection pump at least 2.5 mL/s, followed by 15 mL saline solution. Initially, a non-contrast enhanced series is obtained (“mask”), followed by repeated high temporal resolution, contrast-enhanced series ( $< 20$  seconds/series) during 5 to 10 minutes, in order to evaluate the hemodynamic behavior of the whole prostatic tissue.

The contrast-enhancement peak corresponds to the concentration at which the exponential curve is at its highest. The clearance is defined as the decreasing exponential delay curve. Tumors, particularly in the peripheral zone, demonstrate faster, more intense and short-lasting contrast-enhancement than healthy tissues, mainly due to newly formed vessels with greater

permeability. The combination of early enhancement peak (wash-in) and the presence of clearance (wash-out) are strong indicator of PCa<sup>(21–25)</sup> (Figure 9).

### DIFFUSION-WEIGHTED MRI

Diffusion-weighted MRI may be utilized to increase MRI sensitivity and specificity in the evaluation of prostate tumors, considering that neoplasms usually restrict the diffusion of water molecules. Sequences acquisition should be performed with high  $b$  values (500 to 1000) and always with analysis of images at the apparent diffusion coefficient map for tumor detection. Recent studies have shown that diffusion adds accuracy to MRI in tumors detection, particularly when combined with spectroscopy<sup>(26,27)</sup>.

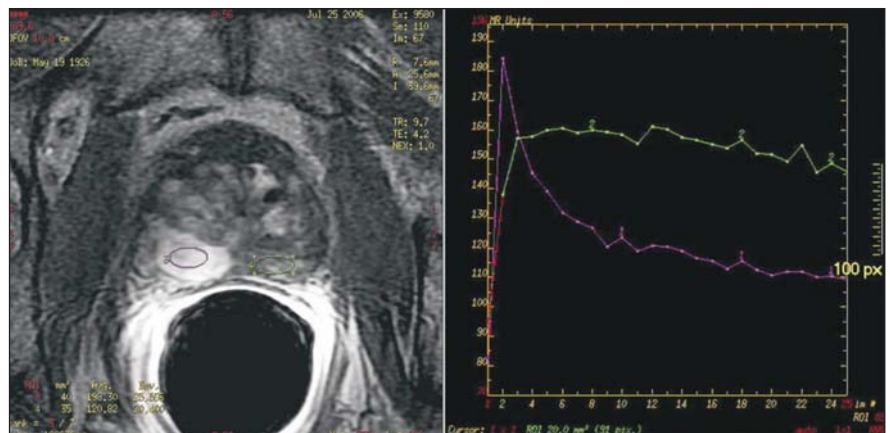


**Figure 9.** Paramagnetic contrast-enhanced MR axial T1-weighted image demonstrating a lesion with early enhancement in the right peripheral zone. Perfusion graph: early enhancement peak, followed by wash-out in the tumor area (purple line) and progressive and persistent enhancement of the normal peripheral zone at left (green line).

## CENTRAL GLAND

Approximately 65% to 74% of tumor nodules originate in the prostatic peripheral zone. Although frequently tumors originated in the central gland present extension to the peripheral zone at the time of the diagnosis, this region may hide PCa in more than 25% of the cases, as demonstrated in specimens from radical prostatectomy<sup>(27)</sup>. Therefore a significant percentage of all PCa's may not be diagnosed in case the radiologist focuses on the peripheral zone only. Prostate cancer detection in the central gland is difficult, as this region presents a high incidence of benign hyperplastic nodules, whose signal intensity is heterogeneous, and sometimes similar to the one in cases of cancer.

One may suspect of tumors in the central gland by the presence of a homogeneously hypointense area on T2-weighted images, with poorly defined or spiculate margins, lenticular shape conditioning the poor definition of the surgical capsule, invasion of the urethra or anterior fibromus-

cular stroma, (choline + creatine)/citrate ratio > 0.7 at spectroscopy, and/or early enhancement peak and prominent clearance at the perfusion study (Figure 10). In contrast, benign prostatic hyperplastic nodules generally present well defined contours, hypointense halo and signal intensity heterogeneity on T2-weighted images<sup>(28,29)</sup>.

## TUMOR DETECTION

### Patients with high PSA levels and negative biopsy

Approximately 66% of patients with PSA levels > 4 ng/ml present negative prostate biopsies, many of them being submitted to rebiopsy with a higher number of fragments. MRI spectroscopy and/or perfusion studies have demonstrated good results in the identification of suspicious foci in patients with clinical-laboratory suspicion of PCa and at least one previous negative biopsy, targeting ultrasound-guided rebiopsy with additional samples of those areas (Figure 11). Accuracy between 80% and 90% has been demonstrated for spec-

troscopy and perfusion in the detection of tumors  $\geq 0.5 \text{ cm}^3$ <sup>(30,31)</sup>.

### Postoperative tumor recurrence

MRI may demonstrate post prostatectomy local recurrence and/or residual tumor, which are seen as soft tissue masses with subtle hyperintense signal on T2-weighted images as compared with the adjacent musculature (Figure 12). The main differentiation to be considered is with postoperative fibrosis, which shows marked hypointensity on T2-weighted images. The main locations for tumor recurrence include: retrovesical (40%), perianastomotic (29%) and in retained seminal vesicles (22%)<sup>(32)</sup>.

### Post-radiotherapy tumor recurrence

Approximately 25% of patients with prostate cancer are treated with radiotherapy, with the rate of PSA recurrence after 5 years ranging from 15% to 67%, depending on each patient's risk.

After radiotherapy, a diffuse reduction in the signal intensity on T2-weighted sequences is observed, as a consequence of

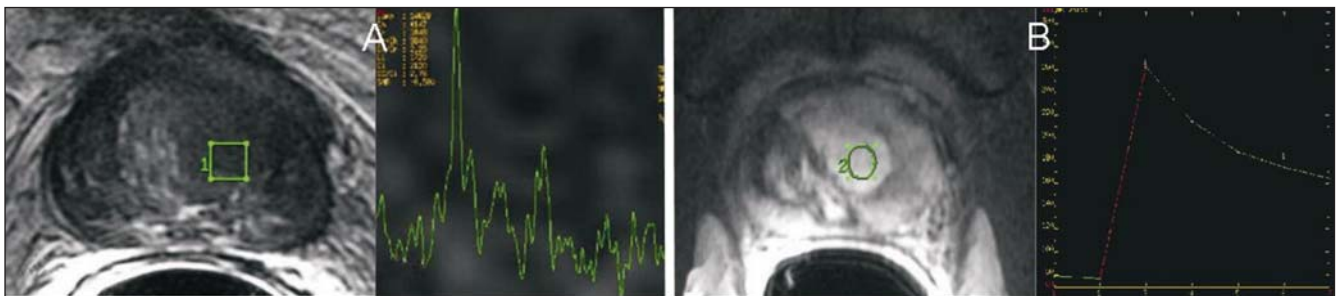


**Figure 10.** MR axial T2-weighted image demonstrating an ill-defined lesion markedly hypointense signal in the central gland at left, with elevated choline peak spectroscopy (A). Perfusion study: neoplastic pattern with early enhancement followed by washout (B). Biopsy revealed PCa.

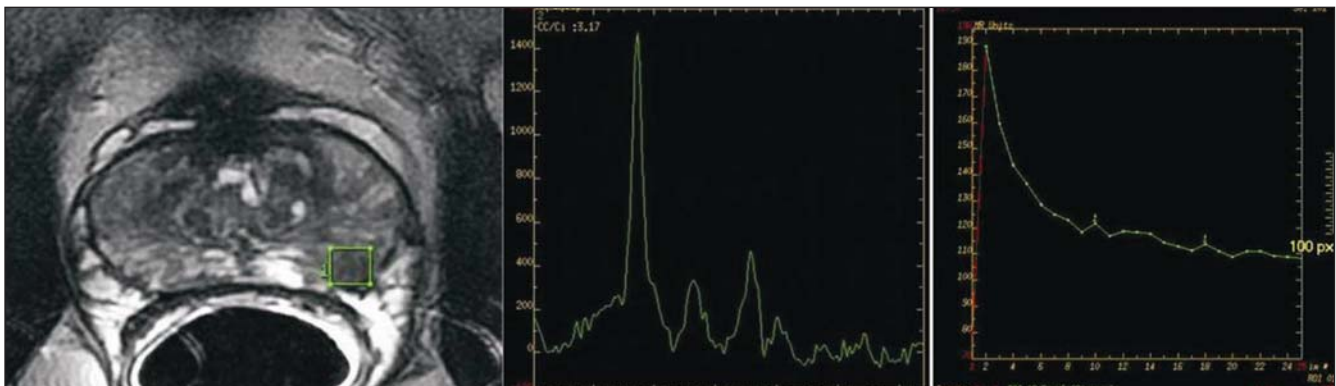


**Figure 11.** Patient with PSA = 7 ng/mL and five previous negative biopsies. MR axial T2-weighted image shows a small lesion with low signal intensity in the middle peripheral zone at left, with increased choline level and decreased citrate level at spectroscopy, and enhancement pattern strongly suggestive of neoplasm at perfusion study. Guided biopsy revealed PCa in this location.

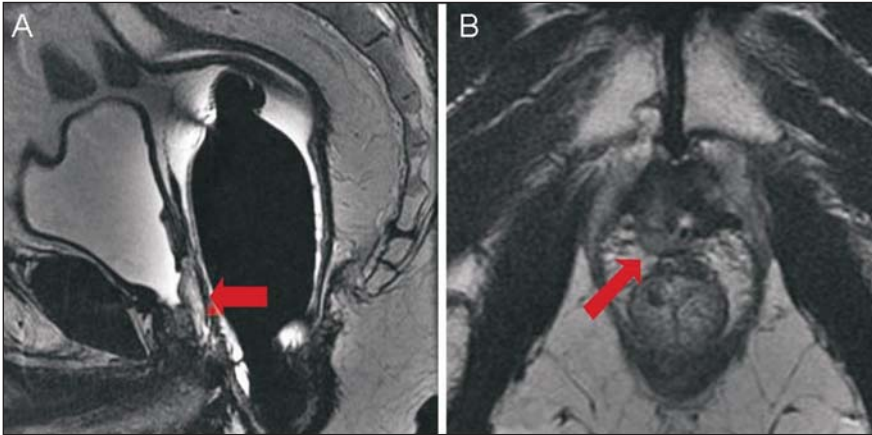


**Figure 12. A:** MR sagittal T2-weighted image demonstrating local post-prostatectomy recurrence in the retrovesical region. **B:** MR axial T2-weighted demonstrating local post-prostatectomy recurrence in the perianastomotic region.

fibrosis and glandular atrophy. The following imaging criteria are adopted in case tumor recurrence is suspected<sup>(33)</sup>:

– MRI criterion: nodular area with marked hypointense signal on T2-weighted sequences.

– Spectroscopy criterion: voxels with a (choline + creatine)/citrate ratio  $\geq 0.5$ ; or any voxel with increased choline levels, when there is too much noise limiting the appropriate individualization of the other metabolites.

## DIFFERENTIAL DIAGNOSIS

Other conditions with hypointense intensity in the peripheral zone on T2-weighted images may mimic prostate cancer, such as hemorrhage, prostatitis, benign prostatic hyperplasia, trauma, other tumors such as lymphoma and sarcoma, among other causes.

Post-biopsy hemorrhage is characterized by hypointense signal on T1-weighted images and variable signal intensity on T2-weighted images. Hemorrhagic foci present a significant decrease 21 days after the procedure, so that this minimum interval should be utilized between biopsy and MRI.

## METHOD LIMITATIONS

MRI is limited as far as small tumors ( $< 0.5 \text{ cm}^3$ ) and low grade tumors (Gleason sum  $< 6$ ) are concerned, and such limitations persist even with the utilization of spectroscopy and perfusion. MRI study is

also impaired in the presence of extensive hemorrhage, hence the already mentioned recommendation of a minimum interval of 21 days between biopsy and MRI.

Artifacts caused by sphincter contraction or body motion may also affect study quality. For this reason, the patient must be carefully instructed on how to avoid these factors prior to the examination. Intestinal peristalsis artifacts can also be minimized with the use of antiperistaltic medication (N-butylscopolamine bromide).

Artifacts may also be found on spectroscopy studies (for example: lipid contamination, partial water peak suppression, low signal-to-noise ratio, susceptibility artifacts affecting the metabolite signals), particularly in patients with prostheses or other metal devices. A correct planning of the spectroscopy sequence, eventually complemented with manual calibration of the sequence, can minimize the effect of such artifacts.

## CONCLUSION

MRI plays a relevant role in the study of the prostate, particularly in the detection and staging of tumors, with the potential to provide valuable information in the therapeutic planning of prostate cancer. Therefore, radiologists must have the knowledge on the indications, potential and limitations of the method.

## REFERENCES

1. Instituto Nacional de Câncer. Estimativas da in-

cidência e mortalidade por câncer no Brasil, 1996-2002. Rio de Janeiro: INCA; 2002.

2. American Cancer Society. Cancer facts and figures. Atlanta: ACS; 2004.
3. Partin AW, Kattan MW, Subong EN, et al. Combination of prostate-specific antigen, clinical stage, and Gleason score to predict pathological stage of localized prostate cancer. A multi-institutional update. *JAMA*. 1997;277:1445-51.
4. Ogura K, Maekawa S, Okubo K, et al. Dynamic endorectal magnetic resonance imaging for local staging and detection of neurovascular bundle involvement of prostate cancer: correlation with histopathologic results. *Urology*. 2001;57:721-6.
5. Wang L, Hricak H, Kattan MW, et al. Prediction of organ-confined prostate cancer: incremental value of MR imaging and MR spectroscopic imaging to staging nomograms. *Radiology*. 2006; 238:597-603.
6. Fütterer JJ, Heijmink SW, Scheenen TW, et al. Prostate cancer: local staging at 3-T endorectal MR imaging – early experience. *Radiology*. 2006; 238:184-91.
7. Heijmink SW, Fütterer JJ, Hambrock T, et al. Prostate cancer: body-array versus endorectal coil MR imaging at 3T – comparison of image quality, localization, and staging performance. *Radiology*. 2007;244:184-95.
8. McNeal JE. The zonal anatomy of the prostate. *Prostate*. 1981;2:35-49.
9. Sobin L. TNM classification of malignant tumors. New York: Willey-Liss; 2002.
10. Carroll PR, Benaron DA, Blackledge G, et al. Third international conference on innovations and challenges in prostate cancer: prevention, detection and treatment. *J Urol*. 2003;170(6 Pt 2):S3-5.
11. Yu KK, Hricak H, Alagappan R, et al. Detection of extracapsular extension of prostate carcinoma with endorectal and phased-array coil MR imaging: multivariate feature analysis. *Radiology*. 1997;202:697-702.
12. Sala E, Akin O, Moskowitz CS, et al. Endorectal MR imaging in the evaluation of seminal vesicle invasion: diagnostic accuracy and multivariate feature analysis. *Radiology*. 2006;238:929-37.
13. Claus FG, Hricak H, Hattery RR. Pretreatment evaluation of prostate cancer: role of MR imaging and 1H MR spectroscopy. *Radiographics*. 2004;24 Suppl 1:S167-80.
14. Kurhanewicz J, Vigneron DB, Hricak H, et al. Three-dimensional H-1 MR spectroscopic imaging of the in situ human prostate with high (0.24-0.7-cm<sup>3</sup>) spatial resolution. *Radiology*. 1996;198: 795-805.
15. Choi H, Ma J. Use of perfluorocarbon compound in the endorectal coil to improve MR spectroscopy of the prostate. *AJR Am J Roentgenol*. 2008; 190:1055-9.
16. Jung JA, Coakley FV, Vigneron DB, et al. Prostate depiction at endorectal MR spectroscopic imaging: investigation of a standardized evaluation system. *Radiology*. 2004;233:701-8.
17. Scheidler J, Hricak H, Vigneron DB, et al. Prostate cancer: localization with three-dimensional proton MR spectroscopic imaging – clinicopathologic study. *Radiology*. 1999;213:473-80.
18. Yu KK, Scheidler J, Hricak H, et al. Prostate cancer: prediction of extracapsular extension with endorectal MR imaging and three-dimensional

- proton MR spectroscopic imaging. *Radiology*. 1999;213:481–8.
19. Zakian KL, Sircar K, Hricak H, et al. Correlation of proton MR spectroscopic imaging with Gleason score on step-section pathologic analysis after radical prostatectomy. *Radiology*. 2005;234:804–14.
  20. Coakley FV, Kurhanewicz J, Lu Y, et al. Prostate cancer tumor volume: measurement with endorectal MR and MR spectroscopic imaging. *Radiology*. 2002;223:91–7.
  21. Fütterer JJ, Engelbrecht MR, Huisman HJ, et al. Staging prostate cancer with dynamic contrast-enhanced endorectal MR imaging prior to radical prostatectomy: experienced versus less experienced readers. *Radiology*. 2005;237:541–9.
  22. d'Arcy JA, Collins DJ, Padhani AR, et al. Informatics in Radiology (infoRAD). *Magnetic Resonance Imaging Workbench: analysis and visualization of dynamic contrast-enhanced MR imaging data*. *Radiographics*. 2006;26:621–32.
  23. Buckley DL, Roberts C, Parker GJ, et al. Prostate cancer: evaluation of vascular characteristics with dynamic contrast-enhanced T1-weighted MR imaging – initial experience. *Radiology*. 2004;233:709–15.
  24. Engelbrecht MR, Huisman HJ, Laheij RJF, et al. Discrimination of prostate cancer from normal peripheral zone and central gland tissue by using dynamic contrast-enhanced MR imaging. *Radiology*. 2003;229:248–54.
  25. Bloch BN, Furman-Haran E, Helbich TH, et al. Prostate cancer: accurate determination of extracapsular extension with high-spatial-resolution dynamic contrast-enhanced and T2-weighted MR imaging – initial results. *Radiology*. 2007;245:176–85.
  26. Reinsberg SA, Payne GS, Riches SF, et al. Combined use of diffusion-weighted MRI and <sup>1</sup>H MR spectroscopy to increase accuracy in prostate cancer detection. *AJR Am J Roentgenol*. 2007;188:91–8.
  27. Haider MA, van der Kwast TH, Tanguay J, et al. Combined T2-weighted and diffusion-weighted MRI for localization of prostate cancer. *AJR Am J Roentgenol*. 2007;189:323–8.
  28. Fütterer JJ, Heijmink SW, Scheenen TW, et al. Prostate cancer localization with dynamic contrast-enhanced MR imaging and proton MR spectroscopic imaging. *Radiology*. 2006;241:449–58.
  29. Akin O, Sala E, Moskowitz CS, et al. Transition zone prostate cancers: features, detection, localization, and staging at endorectal MR imaging. *Radiology*. 2006;239:784–92.
  30. Prando A, Kurhanewicz J, Borges AP, et al. Prostatic biopsy directed with endorectal MR spectroscopic imaging findings in patients with elevated prostate specific antigen levels and prior negative biopsy findings: early experience. *Radiology*. 2005;236:903–10.
  31. Beyersdorff D, Winkel A, Hamm B, et al. MR imaging-guided prostate biopsy with a closed MR unit at 1.5 T: initial results. *Radiology*. 2005;234:576–81.
  32. Sella T, Schwartz LH, Swindle PW, et al. Suspected local recurrence after radical prostatectomy: endorectal coil MR imaging. *Radiology*. 2004;231:379–85.
  33. Pucar D, Shukla-Dave A, Hricak H, et al. Prostate cancer: correlation of MR imaging and MR spectroscopy with pathologic findings after radiation therapy – initial experience. *Radiology*. 2005;236:545–53.